14 Superconductivity and Magnetism

M. Bendele (since January 2014), S. Bosma (until December 2013), Z. Guguchia, L. Howald, H. Keller, G. Pascua, E. Stilp

Visiting scientists: B.I. Kochelaev, R. Puzniak, A. Shengelaya

Emeritus members: K. A. Müller (Honorarprofessor), T. Schneider (Titularprofessor), M. Mali, J. Roos

in collaboration with: Brookhaven National Laboratory (I. Božović, A. Gozar), CEA Grenoble (G. Lapertot, P. Dalmas de Réotier, A. Yaouanc), EPFL Lausanne (D. Pavuna), ETH Zürich (M. Döbeli), Friedrich-Schiller-Universität Jena (F. Schmidl), Kazan State University (B. I. Kochelaev), IFW Dresden (R. Hühne, B. Holzapfel), MPI Stuttgart (J. Köhler, A. Bussmann-Holder, R. Kremer, G. Logvenov), TU Darmstadt (B. Albert, L. Alff), TU Dresden (H.-H. Klauss), Paul Scherrer Institute (K. Conder, R. Khasanov, E. Pomjakushina, A. Suter, H. Luetkens, E. Morenzoni), Polish Academy of Sciences (R. Puzniak, Z. Bukowski), Tbilisi State University (A. Shengelaya), University of Rome La Sapienza (A. Bianconi, N.L. Saini), University of British Columbia, Canada (R.F. Kiefl, W. Hardy)

We report on research projects in the field of high-temperature superconductors (HTS's) and materials with novel electronic properties. Our studies involve various complementary techniques, such as muon-spin rotation (μSR), X-ray absorption spectroscopy XAS, and various standard magnetometry techniques. Here we present some results from our recent investigations on cuprate and iron-based HTS's.

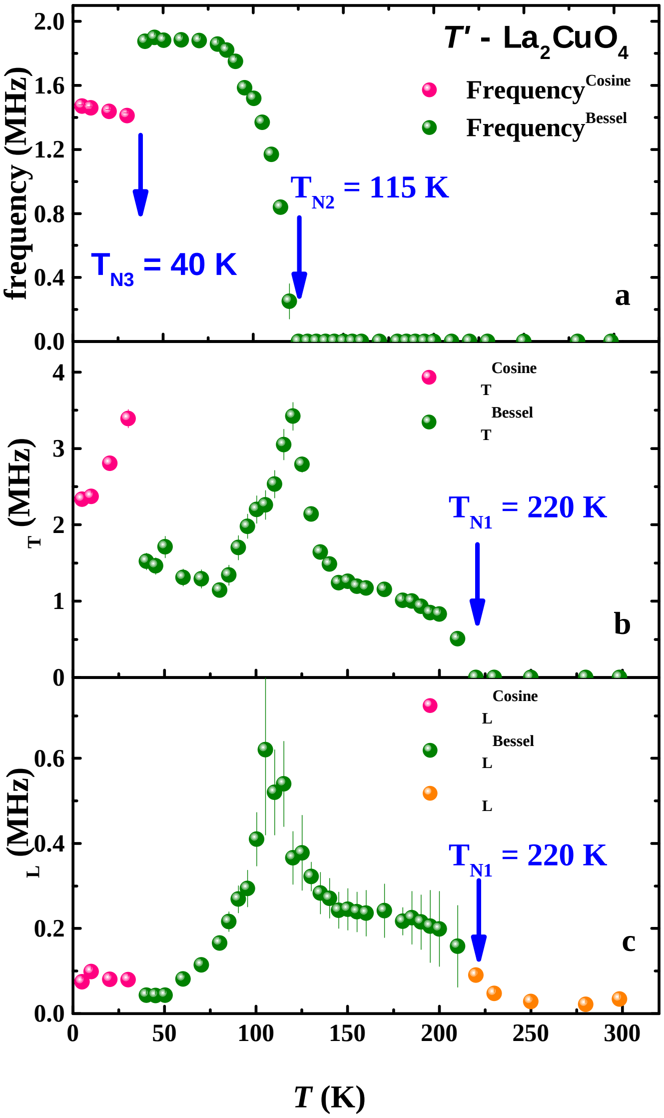

FIG. 14.1 – ZF-μSR parameters for T'-La_2CuO_4: frequency (a), transverse relaxation rate (b), and longitudinal relaxation rate (c) as a function of temperature.

14.1 Magnetic Properties of T'-La_2CuO_4

Recently, for the first time bulk undoped La_2CuO_4 was stabilized in the metastable T'-structure by a low-temperature synthesis method [1, 2]. T'-La_2CuO_4, having no apical oxygen above or below the copper ions of the CuO_2-plane, is the true parent compound of the electron-doped cuprates. In contrast, the hole-doped compounds derived from undoped La_2CuO_4 crystallizes in the T-structure.

The magnetic properties of T'-La_2CuO_4 were investigated by means of muon-spin rotation and relaxation (μSR) measurements as shown in Fig. 14.1. μSR results reveal three characteristic temperature regimes that encompass a quasi-static order with slow magnetic fluctuations between 220 K and 115 K and a true static regime with a broad asymmetric field distribution at the muon site between 115 K and 40 K. At 40 K, an abrupt change to a narrow and symmetric field distribution is observed. These magnetic transitions are marked by arrows in Fig. 14.1.

The investigations on the novel and metastable T'-La_2CuO_4 are of striking significance mainly because our findings in this system had surprisingly revealed series of magnetic transitions even with the nonmagnetic ion La^{3+} [3]. This undoubtedly challenged the common belief that the magnetic interaction between the Cu and the RE system is responsible for, e.g., the spin reorientations observed in T'-Nd_2CuO_4 and thus, also questioned if the observed complex magnetic behavior is generic to all body-centered tetragonal (BCT) cuprates independent of the magnetic state of the RE ion, and if the magnetic transitions might have been overlooked in some compounds, e.g., due to the limitations of simple neutron diffraction experiments. Moreover, T'-La_2CuO_4 revealed a strongly reduced Néel temperature compared to the orthorhombic T-La_2CuO_4 and to other T'-RE_2CuO_4 cuprates such as T'-Nd_2CuO_4 and T'-Pr_2CuO_4. This reduction can be traced back to a ten times decrease in the interlayer coupling possibly due to the missing polarizable lanthanide ion in T'-La_2CuO_4. This low interlayer coupling makes our newly synthesized compound the best realization of a cuprate quasi 2D magnet [3].

[1] R. Hord *et al.*, Phys. Rev. B **82**, 180508 (2010).
[2] R. Hord *et al.*, Z. Anorg. Allg. Chem. **637**, 1114 (2011).
[3] G. Pascua, PhD thesis, Universität Zürich, 2014.

14.2 Magnetic penetration depth and spin order in strained LSCO thin films

Strained thin films of the optimally doped cuprate superconductor $La_{1-x}Sr_xCuO_4$ (LSCO) with a doping of $x = 0.16$ were studied by the low energy muon spin rotation technique (LE-μSR). Several films were grown on different substrates in order to modify the superconducting properties without changing the doping. The LSCO films grown on $SrLaAlO_4$ (LSAO) substrate are under compressive strain (a and b axes of LSAO are $\simeq$ 3% smaller than in LSCO). The 30 and 40 nm thick films have similar superconducting transition temperatures of $T_c \simeq 33$ K. In contrary, $T_c \simeq 14$ K in the 40 nm thin film grown on $SrTiO_3$ (STO) is relaxed with lattice constant as in bulk samples.

Surprisingly, the relaxed film grown on STO shows indications for magnetic order in zero field measurements below $T = 10$ K. Depth dependent measurements revealed that the magnetic fraction of the films is located in the region 4-13 nm below the surface. For the films grown on LSAO substrates a significantly smaller magnetic response was observed below 5 K.

The superconducting properties were studied by field dependent measurements in the vortex state at low temperatures. The muon relaxation rate σ measures the field inhomogeneities in the sample arising from the formation of the vortex lattice. Theoretically, it has its maximum where the distance between the vortices is of the order of the effective magnetic penetration depth [1]. The variation in the position of the maximum between films of equal thickness grown on different substrates seen in Fig. 14.2 corresponds to the expectation for samples with different T_c [2]. In contrary, the variation with film thickness exceeds from far the expectation associated with the variation of effective magnetic penetration depth. The increase of σ observed at high fields consistently for all the samples investigated is ascribed to a field induced ordering of magnetic moments in at least some fraction of the LSCO films. Since a magnetic layer was found close to the surface interface of one film and since some magnetic fraction can be generally induced under magnetic field, we might speculate the existence of different domains, with superconductivity never occurring close to the surface interface and leading to a smaller effective film thickness for superconductivity. A non-superconducting layer of constant thickness with (zero) field induced moments ordering would explain all the curves of Fig. 14.2.

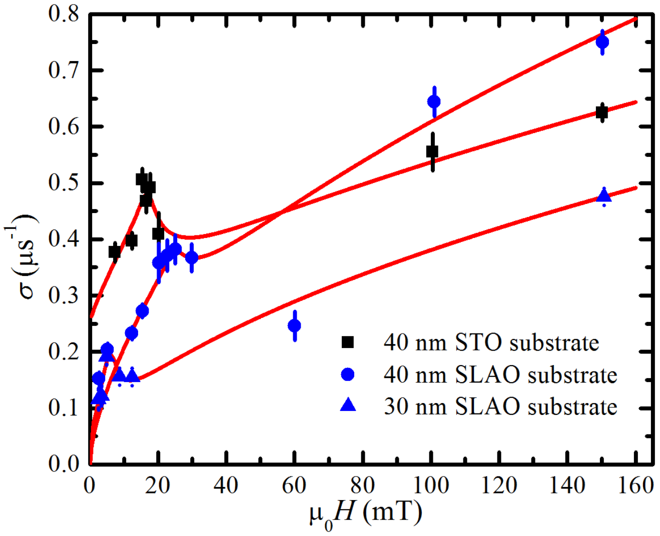

FIG. 14.2 – Magnetic field dependence of the muon relaxation rate σ in LSCO thin films grown on different substrates. The full lines are guides to the eyes.

[1] E. Brandt *et al.*, Phys. Rev. B **71**, 014521 (2005).
[2] Y. J. Uemura *et al.*, Phys. Rev. Lett. **62**, 2317 (1989).

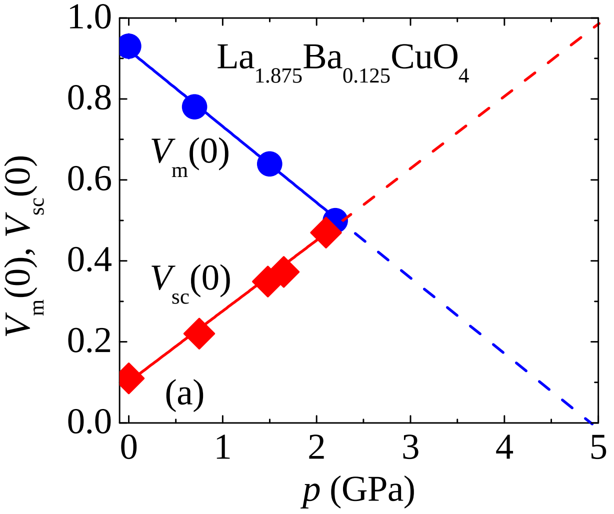

FIG. 14.3 – The pressure dependence of the zero-temperature limit of the magnetic and the SC volume fractions, $V_m(0)$ and $V_{sc}(0)$, respectively, of LBCO-1/8. Solid lines are linear fits to the data [5].

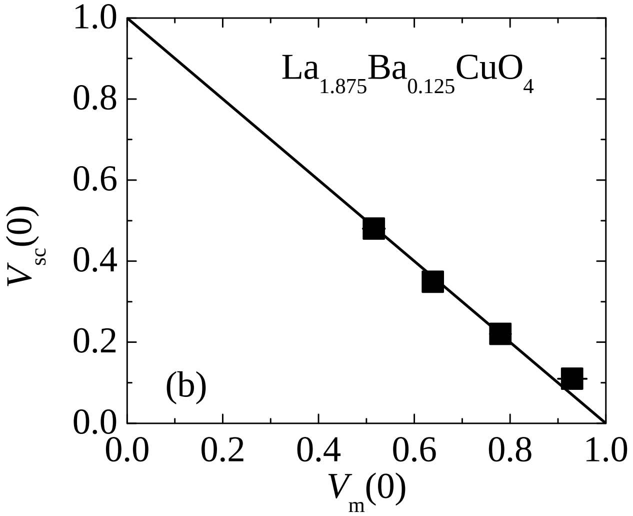

FIG. 14.4 – $V_{sc}(0)$ vs. $V_m(0)$. The straight line is drawn between a hypothetical situation of a fully magnetic ($V_m(0)$ = 1) and a fully SC state ($V_{sc}(0)$ = 1) [5].

14.3 Tuning the static spin-stripe phase and superconductivity in $La_{2-x}Ba_xCuO_4$ ($x = 1/8$) by hydrostatic pressure

$La_{2-x}Ba_xCuO_4$ (LBCO) was the first cuprate system where high-T_c superconductivity was discovered [1]. In LBCO the superconducting (SC) transition temperature T_c has a deep minimum at $x = 1/8$ [2], which is known as the 1/8 anomaly. Here a structural transition from a low-temperature orthorhombic (LTO) to a low-temperature tetragonal (LTT) phase was observed [3]. Neutron diffraction experiments revealed two-dimensional charge and spin order in $La_{1.48}Nd_{0.4}Sr_{0.12}CuO_4$ [4]. It was proposed [4] that the density of the dopant induced charge carriers modulates spatially in a periodic fashion forming a self-organized alternating array of charge and spin stripes and that the carriers are pinned by the lattice modulation in the LTT phase, and T_c is suppressed. Experimental results and theoretical considerations show that in the stripe phase charge and spin order appear to be a generic feature of the cuprates. However, the role of stripes for superconductivity in cuprates is still unclear at present.

Our recent studies of magnetism and superconductivity in LBCO-1/8 as a function of pressure revealed an unusual interplay between spin order and bulk superconductivity [5]. With increasing pressure the spin order temperature and the size of the ordered moment are not changing significantly. However, application of hydrostatic pressure leads to a remarkable decrease of the magnetic volume fraction $V_m(0)$ (see Fig. 14.3). Simultaneously, an increase of the SC volume fraction $V_{sc}(0)$ occurs. Furthermore, it was found that $V_m(0)$ and $V_{sc}(0)$ at all p are linearly correlated: $V_m(0) + V_{sc}(0) \simeq 1$ (Fig. 14.4). This is an important new result, indicating that the magnetic fraction in the sample is directly converted to the SC fraction with increasing pressure. The present results provide evidence for a competition between bulk superconductivity and static magnetic order in the stripe phase of LBCO-1/8, and that static stripe order and bulk superconductivity occur in mutually exclusive spatial regions.

[1] J.G. Bednorz *et al.*, Z. Phys. B **64**, 189 (1986).
[2] A.R. Moodenbaugh *et al.*, Phys. Rev. B **38**, 4596 (1988).
[3] J.D. Axe *et al.*, Phys. Rev. Lett. **62**, 2751 (1989).
[4] J.M. Tranquada *et al.*, Nature **375**, 561 (1995).
[5] Z. Guguchia *et al.*, New Journal of Physics **15**, 093005 (2013).

14.4 Gold nanoparticles on $YBa_2Cu_3O_{7-\delta}$ thin films

Disorder within cuprate high temperature superconductors can strongly affect its superconducting properties. In $YBa_2Cu_3O_{7-\delta}$, for instance, the substitution of Cu atoms by metal ions decreases the superconducting transition temperature T_c [1]. Surprisingly, doping with gold showed the opposite effect: if 10 % of Cu from the Cu-O chains is replaced by Au in single-crystal $YBa_2Cu_3O_{7-\delta}$, T_c is increased by 1.5 K [2].

Recently, Au nanoparticles have been incorporated in $YBa_2Cu_3O_{7-\delta}$ thin films to improve the pinning properties. Beside the expected increase in the critical current density j_c (from $4 \cdot 10^7$ A/cm^2 to $6 \cdot 10^7$ A/cm^2 at 10 K) a higher T_c was observed as well [3]. We utilized low-energy muons to investigate the microscopic changes on

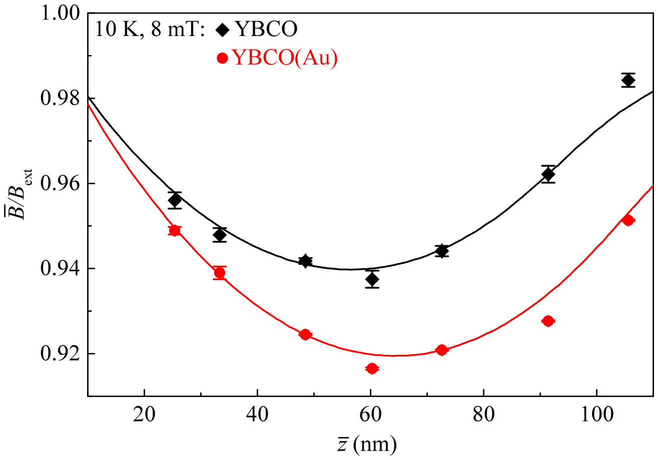

FIG. 14.5 – The average local magnetic field normalized to the applied field $\bar{B}/B_{\mathrm{ext}}$ versus the mean muon implantation depth $\bar{z}$ measured perpendicular to the film surface for thin-film YBCO and YBCO(Au) by low-energy muon spin rotation [4]. The solid lines represent the results of the global fits taking 7 μSR spectra at different $\bar{z}$ into account. The data points are determined from single spectra fits.

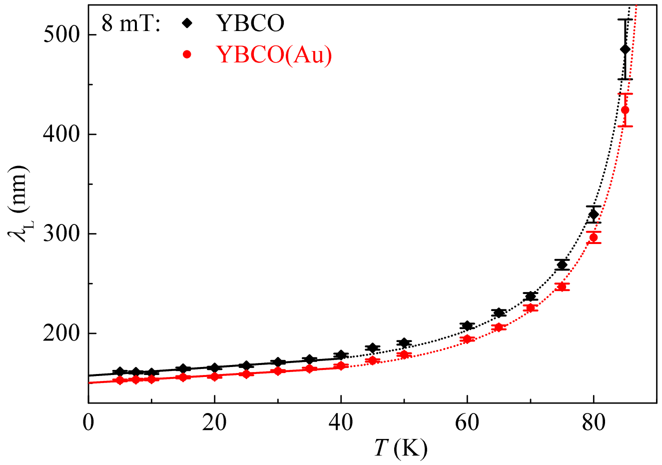

FIG. 14.6 – The London penetration depth λ_{L} versus temperature T for thin-film YBCO and YBCO(Au) determined by low-energy muon spin rotation [4]. The corresponding solid lines are linear fits to the data in the range $5-35$ K. The dotted lines are fits to a power law.

the superconducting properties due to the Au nanoparticles [4]. Therefore, slowed down muons have been implanted in different depths into the sample to investigate the magnetic screening profile $B(z)$ in the Meissner state. By determining the London penetration depth λ_{L} direct conclusion on the superfluid density n_{s} could be drawn, since they are related via the effective mass m^*.

We investigated two sets of thin-film samples, one with [YBCO(Au)] and one without (YBCO) Au nanoparticles. We observed a shift of $\Delta T_{\mathrm{c}} = 0.6(3)$ K between YBCO(Au) and YBCO, determined by resistivity measurements [4]. The magnetic penetration profile $\bar{B}(\bar{z})$, depicted in Fig. 14.5, has the expected shape of a cosh (exponential decay from both interfaces), according to the London equation. The YBCO(Au) samples screen the magnetic field stronger and therefore exhibit a lower London penetration depth. This reduction of λ_{L} may be due a lowered defect density, originating from a condensation of defects at the Au nanoparticles. Diffusion of Au into the $YBa_2Cu_3O_{7-\delta}$ structure may also influence λ_{L} as well as T_{c}.

The temperature dependence of λ_{L} in YBCO(Au) is similar to pristine YBCO in terms of shape and slope, but the absolute scale is shifted (see Fig. 14.6). The penetration depth increases linearly with temperature up to 35 K, which is characteristic for d-wave pairing. At higher temperatures $\lambda_{\mathrm{L}}(T)$ is described by a power law yielding a higher T_{c} for YBCO(Au), in agreement with the resistivity measurements. This implies that incorporated Au nanoparticles do not affect the fundamental properties, like the pairing behavior and the size of the superconducting gap, but the quality of thin-film $YBa_2Cu_3O_{7-\delta}$ is improved remarkably due to the reduced disorder.

[1] L. Shlyk *et al.*, Physica C **377**, 437 (2002)
[2] M. Z. Cieplak *et al.*, Appl. Phys. Lett. **57**, 934 (1990).
[3] C. Katzer *et al.*, Supercond. Sci. Technol. **26**, 125008 (2013).
[4] E. Stilp *et al.*, Phys. Rev. B **89**, 020510(R) (2014).

14.5 Pressure effects in iron-chalcogenides

Among the iron-based superconductors the iron chalcogenide system exhibits the highest superconducting transition temperatures T_{c} [1]. Due to their simple structure they may act as a model system to gain insight into the mechanism of high temperature superconductivity in the iron-based materials. Whereas several authors propose a purely electronic model for the appearance of superconductivity (see, e.g., Refs. [2]), experimental isotope exchange studies demonstrate the significant influence of the lattice in the Cooper pairing [3].

Despite being the simplest among the Fe-based superconductors, the iron chalcogenides are among the most fascinating compounds: intercalation or application of pressure leads to a large increase of T_{c} and highly unexpected and unique effects in the superconducting and magnetic properties. The antiferromagnetic FeTe was predicted to become superconducting under hydrostatic pressure. However, a ferromagnetic ground state requiring similar electronic properties close to the Fermi level as the superconducting ground state is realized. Application of chemical pressure by partial substitution of Se by Te first leads to an increase of $T_c \simeq 14$ K before the material develops an antiferromagnetic ground state after crossing a coexistence region, in which both electronic ground states coexist.

Considering the above mentioned pressure effects in the iron chalcogenides, it is rather surprising that we find in $FeSe_{0.5}Te_{0.5}$ under pressure a moderate increase of T_c from $\simeq 14$ to $\simeq 23$ K until $p \simeq 2.2$ GPa followed by a smooth decrease. The X-ray absorption spectroscopy (XAS) measurements presented in Fig. 14.7 (a) and (b) at the Fe and Se K-edges reveal that compression affects the local structure significantly and in a discontinuous manner across the known tetragonal to monoclinic structural phase transition at $p_S \simeq 3$ GPa [4], whereas it does not have an analogous important effect on the electronic structure. Interestingly, both the superconducting volume fraction and T_c are decreasing as soon as the crystallographic structure changes, i.e. above p_S, underlining the importance of the lattice for the superconducting and magnetic properties (see Fig. 14.7 (c)). However, since the electronic structure shows no significant changes across the structural transition, the modifications in the superconducting properties in this system arise by structural effects.

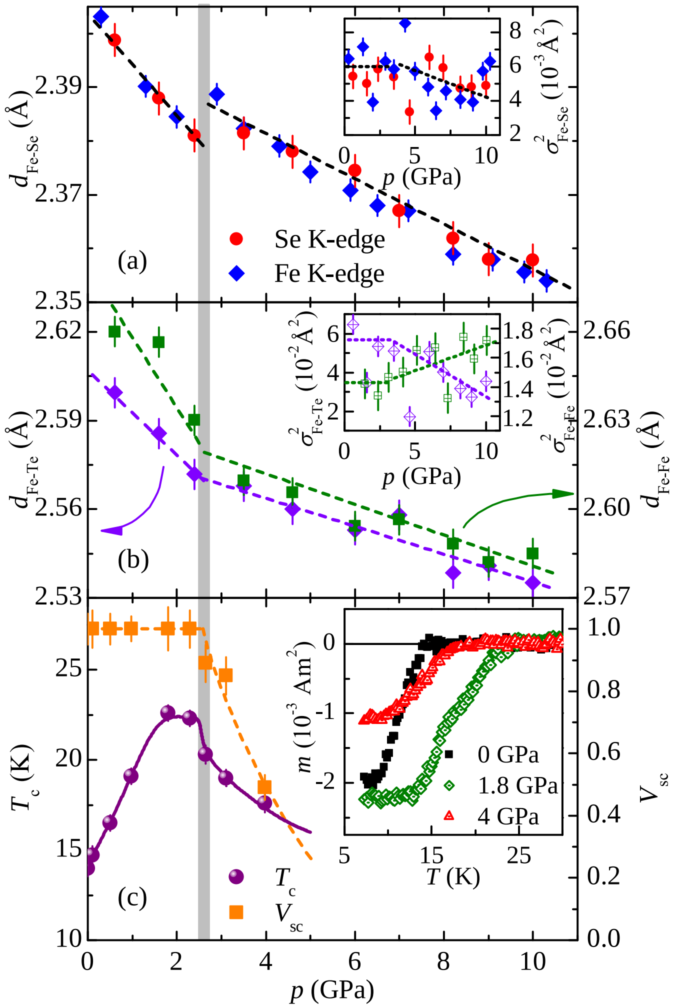

FIG. 14.7 –
(a) Pressure dependence of the Fe-Se bond length $d_{\text{Fe-Se}}$ of $FeSe_{0.5}Te_{0.5}$ at room temperature obtained from Se K-edge and Fe K-edge measurements.
(b) The left and right axes show the pressure evolution of the Fe-Te and Fe-Fe distances.
The insets in (a) and (b) show the corresponding Debye-Waller factors σ^2 representing the disorder of the bonds.
(c) Pressure dependence of the superconducting transition temperature T_c (left axis) and the superconducting volume fraction (right axis). The inset shows magnetization measurements for selected pressures.
The gray bar at $p \simeq 3$ GPa indicates the structural phase transition. The dashed lines are a guide to the eyes.

[1] S. He, *et al.*, Nature Mater. **12**, 605 (2013).

[2] P. J. Hirschfeld, *et al.*, Rev. Prog. Phys. **74**, 124508 (2011); R. M. Fernandes, *et al.*, Nature Physics **10**, 97 (2014).

[3] R. H. Liu, *et al.*, Nature **459**, 64 (2009); R. Khasanov, *et al.*, Phys. Rev. B **82**, 212505 (2010); R. Khasanov, *et al.*, New J. Phys. **12**, 073024 (2010);

[4] N. C. Gresty, *et al.*, J. Am. Chem. Soc. **131**, 16944 (2009).